CRISPR/Cas9-based gene targeting using synthetic guide RNAs enables robust cell biological analyses

Kuan-Chung Su[a], Mary-Jane Tsang[a], Neil Emans[b], and Iain M. Cheeseman[a,c,*]
[a]Whitehead Institute for Biomedical Research, Cambridge, MA 02142; [c]Department of Biology, Massachusetts Institute of Technology, Cambridge, MA 02142; [b]Persomics USA, Weston, MA 02493

ABSTRACT **A key goal for cell biological analyses is to assess the phenotypes that result from eliminating a target gene. Since the early 1990s, the predominant strategy utilized in human tissue culture cells has been RNA interference (RNAi)-mediated protein depletion. However, RNAi suffers well-documented off-target effects as well as incomplete and reversible protein depletion. The implementation of CRISPR/Cas9-based DNA cleavage has revolutionized the capacity to conduct functional studies in human cells. However, this approach is still underutilized for conducting visual phenotypic analyses, particularly for essential genes that require conditional strategies to eliminate their gene products. Optimizing this strategy requires effective and streamlined approaches to introduce the Cas9 guide RNA into target cells. Here we assess the efficacy of synthetic guide RNA transfection to eliminate gene products for cell biological studies. On the basis of three representative gene targets (KIF11, CENPN, and RELA), we demonstrate that transfection of synthetic single guide RNA (sgRNA) and CRISPR RNA (crRNA) guides works comparably for protein depletion as cell lines stably expressing lentiviral-delivered RNA guides. We additionally demonstrate that synthetic sgRNAs can be introduced by reverse transfection on an array. Together, these strategies provide a robust, flexible, and scalable approach for conducting functional studies in human cells.**

Monitoring Editor
David G. Drubin
University of California, Berkeley

Received: Apr 5, 2018
Revised: Jul 16, 2018
Accepted: Jul 26, 2018

INTRODUCTION

CRISPR/Cas9-based gene knockouts provide a powerful tool for functional studies, overcoming many limitations of RNA interference (RNAi) (Shalem *et al.*, 2015). This approach has been used successfully to generate targeted gene knockouts for individual factors (Cho *et al.*, 2013; Mali *et al.*, 2013; McKinley and Cheeseman, 2017) or to conduct large-scale functional analyses to define factors required for optimal cell growth under specific conditions based on guide barcode enrichment or depletion (Shalem *et al.*, 2014; Wang *et al.*, 2014, 2015, 2017; Morgens *et al.*, 2016; Tzelepis *et al.*, 2016). The wealth of screens conducted using pooled Cas9-based knockout strategies has provided extensive information regarding the contribution of each individual gene to cellular fitness and also how this requirement changes under different perturbations, such as drug treatment (Jost *et al.*, 2017; Zimmermann *et al.*, 2018). However, such pooled screens do not reveal the specific consequences of a knockout or the function of a given gene in different cellular processes. The use of CRISPR/Cas9 for phenotypic cell biological studies that rely on visual microscopy-based outputs remains less common and would complement these pooled barcode-based studies. To facilitate the ability to conduct CRISPR/Cas9-based targeting and cell biological studies on a larger scale, our goal was to compare different guide RNA types and delivery approaches for cell biological analyses of Cas9-mediated knockouts.

Given the critical requirements for the proteins that function in core cell biological processes, it is important to generate robust strategies to conditionally eliminate these essential genes. For our previous work (McKinley *et al.*, 2015; McKinley and Cheeseman, 2017), we generated human cell lines stably expressing a single

This article was published online ahead of print in MBoC in Press (http://www.molbiolcell.org/cgi/doi/10.1091/mbc.E18-04-0214) on August 9, 2018.

*Address correspondence to: Iain M. Cheeseman (icheese@wi.mit.edu).

Abbreviations used: CCD, charge-coupled device; crRNA, CRISPR RNA; EGTA, ethylene glycol-bis(β-aminoethyl ether)-*N,N,N′,N′*-tetraacetic acid; FBS, fetal bovine serum; FITC, fluorescein isothiocyanate; PIPES, piperazine-*N,N′*-bis(2-ethanesulfonic acid); RNAi, RNA interference; sgRNA, single guide RNA; tracrRNA, *trans*-activating crRNA.

guide RNA (sgRNA) targeting a gene of interest (integrated by lentiviral infection), together with a doxycycline-inducible version of Cas9. On induction of Cas9, the Cas9/sgRNA complex is targeted to the gene of interest and generates double-stranded DNA breaks that are repaired in an error-prone manner until the target site is eliminated to prevent further cutting. This typically results in small deletions, with the majority of these creating frame shifts that eliminate protein production. Although not all of the cells within a population will fully eliminate the target protein, we have found this strategy to be highly effective for generating potent and irreversible gene knockouts with a substantial proportion of cells displaying the knockout phenotype shortly after Cas9 induction (McKinley *et al.*, 2015; McKinley and Cheeseman, 2017). However, the need to construct the sgRNA plasmid, generate lentivirus, and select a stable cell line creates significant limitations for the tractability and scalability of this approach. As an alternative strategy to utilize Cas9 to generate inducible gene knockouts, we sought to compare the lentiviral-based system with the transfection of exogenous guide RNAs.

Targeting Cas9 to a gene locus requires both complementarity to the target DNA sequence and loading into the Cas9 complex. In endogenous bacterial type II CRISPR/Cas systems, the targeting RNA (CRISPR RNA; crRNA) and Cas9 loading component (*trans*-activating crRNA; tracrRNA) are encoded by distinct elements, which after processing then anneal to form the intact molecule that is loaded onto the Cas9 protein (Deltcheva *et al.*, 2011). To simplify this system and facilitate expression of an effective targeting guide RNA in cells, engineered CRISPR/Cas9 systems typically combine the crRNA and tracrRNA components into a single extended RNA sequence, termed a single guide RNA or sgRNA (Jinek *et al.*, 2012; Cong *et al.*, 2013). As a synthetic version, commercial sources provide the RNA as either a full-length complete sgRNA comparable to that expressed by the lentiviral vector or as a two-component system comprising the targeting crRNA sequence and a scaffold tracrRNA for loading into the Cas9 complex.

We assessed the transfection of synthetic sgRNAs and crRNAs across multiple distinct conditions. Our work demonstrates that transfection of synthetic guide RNAs results in potent and high-frequency gene knockout, thus providing an effective strategy that will facilitate diverse cell biological studies.

RESULTS AND DISCUSSION

Transfection of synthetic Cas9 guides provides an effective strategy for functional studies

To evaluate the effectiveness of the synthetic RNA guides, we chose three gene targets with diverse behaviors: 1) the kinesin-5 KIF11 (Mayer *et al.*, 1999), a motor protein essential for bipolar spindle formation; 2) the kinetochore component CENPN, which is required for chromosome alignment and segregation (McKinley *et al.*, 2015); and 3) the NF-kB subunit RELA (Ruben *et al.*, 1991; Schmid *et al.*, 1991), which is not required for cell growth, but whose depletion can be assessed by immunofluorescence and flow cytometry. In each case, we compared the behavior of a lentiviral-generated cell line stably expressing an sgRNA targeting the gene of interest to that of cells transfected with the identical guide sequence, delivered either as a synthetic sgRNA or crRNA using a standard RNA transfection protocol developed for RNAi (see *Materials and Methods*). The same parental cell line—a HeLa cell line containing an inducible Cas9 construct stably integrated into the genome (McKinley *et al.*, 2015)—was used in all conditions to provide a direct comparison of efficacy. The synthetic guides tested were obtained from two different manufacturers and applied at the recommended concentrations (15 nM for ThermoFisher and 25 nM for Dharmacon). In addition, we analyzed the behavior of sgRNAs that we transcribed using a commercial in vitro transcription kit (Takara). In the case of the exogenous RNA guides, the corresponding synthetic guides were transfected 12–20 h after Cas9 induction.

In all cases, we found that transfection of synthetic guide RNA was effective in eliminating the target gene (Figure 1). Importantly, the efficacy of the synthetic full-length sgRNA was comparable to that of cell lines stably expressing the transgenic sgRNA sequences using a lentiviral construct. Targeting the KIF11 gene with synthetic sgRNAs resulted in a potent mitotic arrest with monopolar spindles in 90 ± 6.2% (Dharmacon) and 89 ± 2% (ThermoFisher) of mitotic cells (Figure 1, A and C, and Supplemental Figure S1A). We also observed depletion of the Kif11 protein in those cells by immunofluorescence (Supplemental Figure S1A). A similar frequency of mitotic cells with monopolar spindles (82 ± 3.6%) was obtained with the lentiviral sgRNA-expressing cell line. Next, we assessed the CRISPR-mediated knockout of CENPN, which results in mitotic cells with misaligned chromosomes and/or multipolar or collapsed spindles (Supplemental Figure S1B). We found that the fraction of mitotic cells with the described phenotype was comparable for both the stable cell line and sgRNA-transfected cells (70.7 ± 8% vs. 68.25 ± 7.4% for Dharmacon sgRNA or 74.95 ± 12% for ThermoFisher sgRNA) (Figure 1, B and D). Finally, we assessed RELA depletion by immunofluorescence (Figure 1F) and flow cytometry (Figure 1E and Supplemental Figure S1) and obtained similar results to the other two gene targets. In this case, 48 ± 2% of cells expressing the lentiviral sgRNA were RELA negative, compared with 43.9 ± 8.4% (Dharmacon) and 41.5 ± 3.8% (ThermoFisher) for the transfected synthetic sgRNAs (Figure 1, E and F). Overall, we observed similar behavior for synthetic sgRNAs obtained from the two different commercial providers. We also tested in vitro transcribed sgRNAs and obtained mixed results ranging from poor efficiency for RELA to comparable efficiency to the commercial sgRNAs for KIF11 and CENPN (Figure 1). Thus, transfection of synthetic guide RNAs provides an effective strategy to conduct phenotypic analyses of protein depletion, comparable to cell lines stably expressing guide RNAs by lentiviral-mediated infection.

Comparison of sgRNAs and crRNAs for functional studies using Cas9

Synthetic RNA guides are commercially available as a full-length sgRNA sequence or a shorter crRNA that is combined with a tracrRNA prior to transfection. In term of cost, sgRNAs are more expensive than crRNAs due to their increased length. Thus, we sought to compare the effectiveness of sgRNA versus crRNA for our specific gene targets (KIF11, CENPN, and RELA). In all cases, the crRNA behaved less efficiently than the corresponding sgRNA (Figure 1). In addition, cells transfected with either sgRNA or crRNA showed marked differences in their knockout kinetics. For these experiments, we focused solely on synthetic RNA guides obtained from ThermoFisher. For KIF11, at 30 h posttransfection, 60.3 ± 12.3% of mitotic cells transfected with the crRNA displayed monopolar spindles, compared with 90.3 ± 4% with sgRNA transfection (Figure 2A). This suggests a more pronounced delay between RNA transfection and manifestation of the knockout phenotype with the crRNA. However, if given enough time, the crRNA-transfected cells ultimately displayed a similar extent of gene knockout as sgRNA-transfected cells (92 ± 1.7% for crRNA vs. 89.7 ± 0.6% for sgRNA when assessed at 48 h posttransfection). Interestingly, although the same delay in knockout efficiency is observed for CENPN crRNA (Figure 2B), the crRNA-transfected cells displayed less mitotic cells with misaligned chromosomes and/or multipolar or collapsed

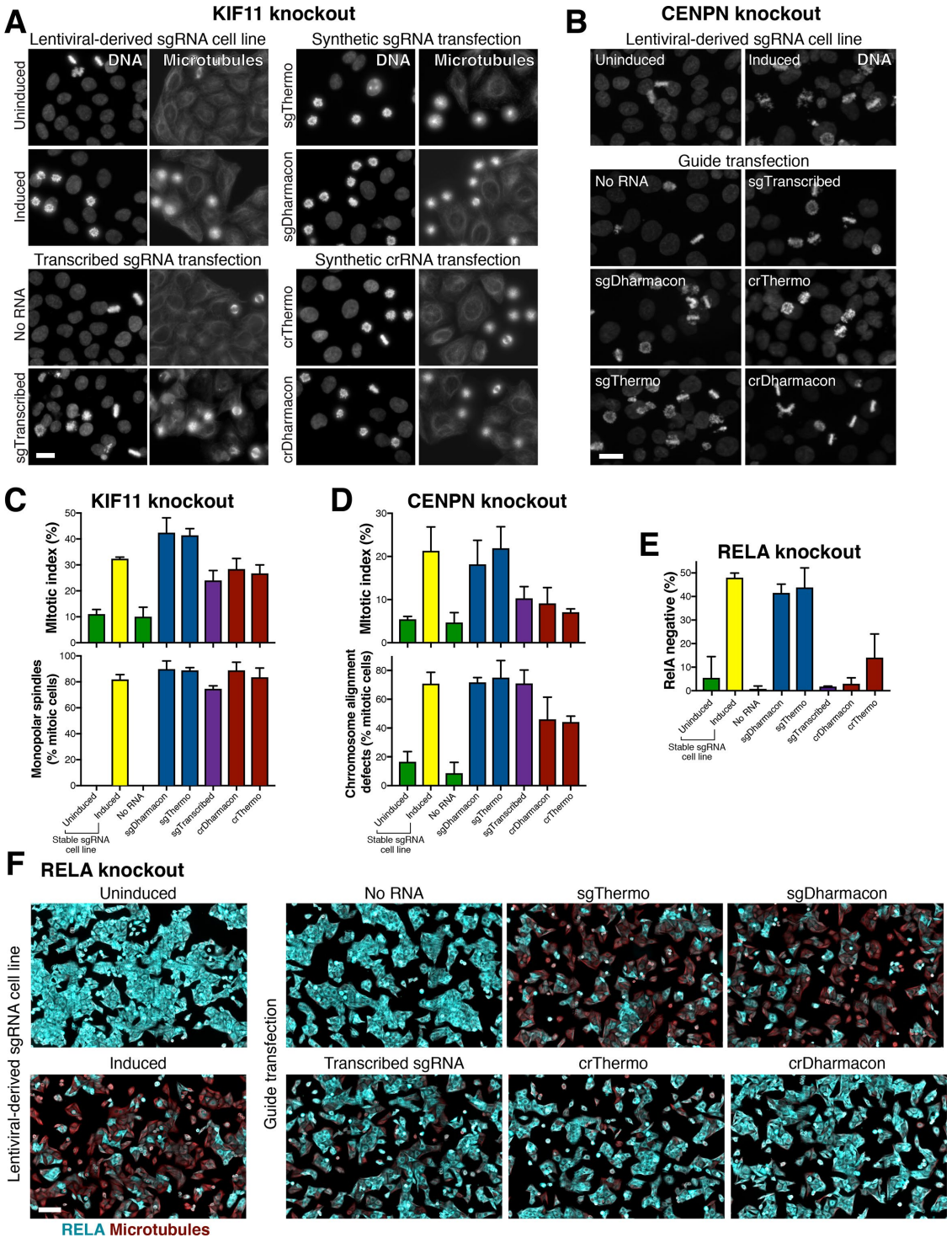

FIGURE 1: Transfection of synthetic guide RNAs is effective to generate potent gene knockouts for cell biological analyses. (A, B) Fluorescence images of cells with RNA guides targeting KIF11 (A) or CENPN (B), stained for DNA and/or microtubules as indicated. Mitotic index indicates the percentage of total cells in mitosis. For KIF11, Cas9 was induced for 66–68 h before imaging and the synthetic/transcribed RNAs were transfected 48 h before imaging and analysis. For CENPN, both Cas9 induction and RNA transfection were performed 60 h before imaging and analysis. (C–E) Quantification of knockout phenotypes for KIF11 (C) and CENPN (D) by immunofluorescence and RELA (E) by flow cytometry. The number of cells scored and statistical comparisons performed can be found in Supplemental Tables S1 and S2, respectively. Data are displayed as mean with error bars indicating SD. (F) Immunofluorescence images of cells with RNA guide targeting RELA and stained for RELA (cyan) and microtubules (red). Cas9 expression was induced for 84 h before imaging and the synthetic/transcribed RNAs were transfected 72 h before imaging and analysis. Scale bar = 20 μm (A, B) or 100 μm (F).

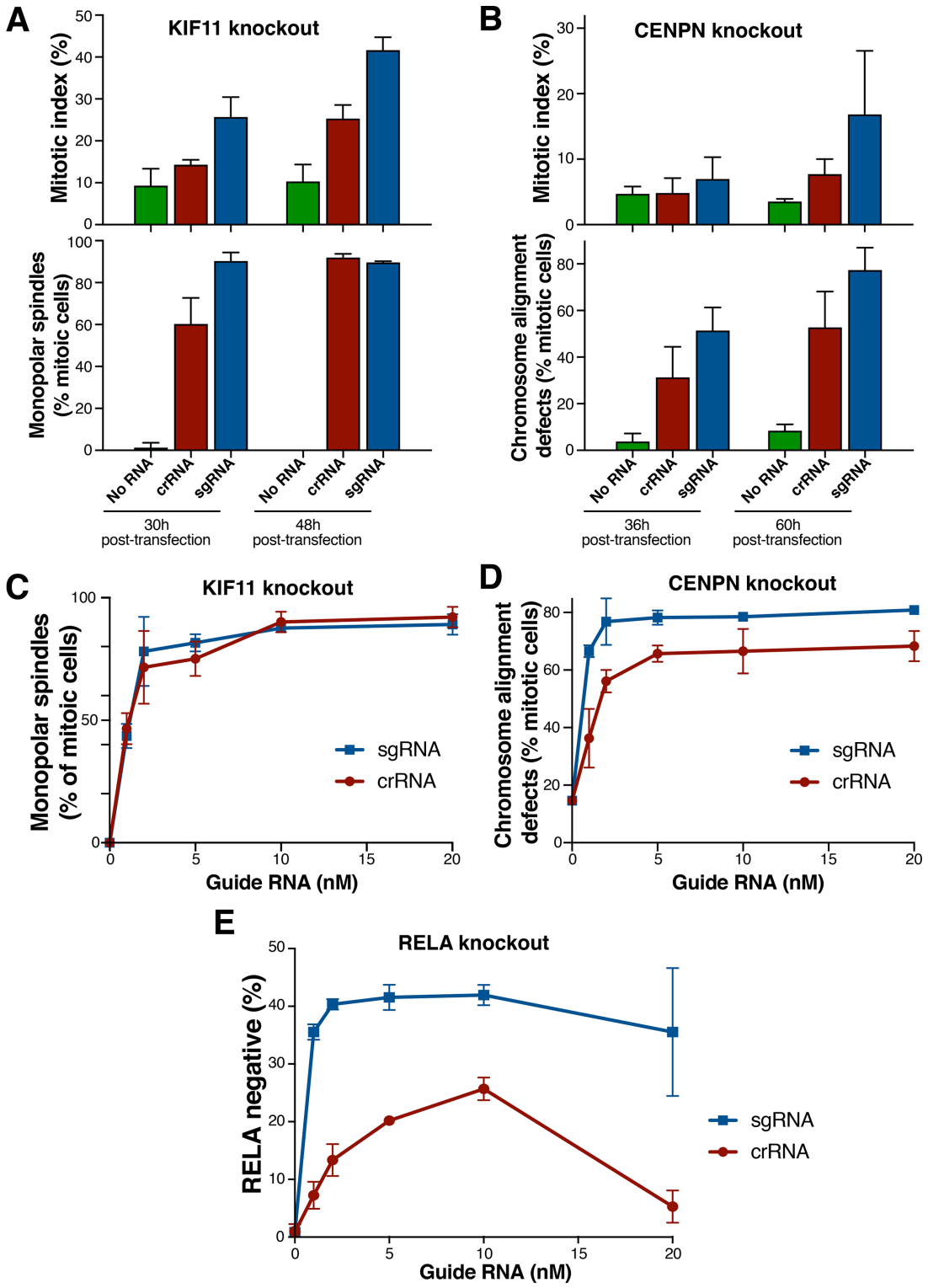

FIGURE 2: Comparison of efficiency of crRNAs and sgRNAs for gene disruption. (A, B) Quantification of knockout phenotype for cells transfected with 15 nM synthetic crRNA or sgRNA targeting KIF11 (A) or CENPN (B), imaged at the indicated times posttransfection. Mitotic index indicates the percentage of total cells in mitosis. Cas9 expression was induced 18–20 h before transfection for KIF11 or simultaneously with RNA transfection for CENPN. Number of cells counted and statistical comparisons performed can be found in Supplemental Tables S1 and S2. (C–E) Titration of RNA guide concentrations for crRNA and sgRNA targeting KIF11 (C), CENPN (D), and RELA (E). Cells transfected with KIF11-targeting crRNA and sgRNA were treated as described above and imaged at 48 and 30 h posttransfection, respectively, to catch the peak knockout period for each synthetic guide. Cells transfected with CENPN or RELA RNA guides were treated as described in Figure 1 and analyzed at 60 or 72 h posttransfection, respectively. Quantification of the knockout phenotypes was done using immunofluorescence (KIF11/CENPN) and flow cytometry (RELA). Data are displayed as mean with error bars indicating SD.

spindles (52.8 ± 15.3%) compared with sgRNA-transfected cells (77.4 ± 9.5%), even at 60 h posttransfection. One possibility is that a longer time posttransfection is required for the CENPN crRNA to be fully effective. Overall, crRNAs appear to be less effective than the corresponding sgRNAs but still result in gene knockout and the manifestation of the phenotype in at least a subset of cells.

To further compare the effectiveness of the sgRNAs and crRNAs, we titrated the concentration of the transfected guide RNAs from 1 to 20 nM and assessed the described knockout phenotypes at selected intervals posttransfection. For KIF11, the sgRNA and crRNA displayed similar knockout efficiency over the range of concentrations tested, with no further increase in the fraction of mitotic cells with monopolar spindles at concentrations higher than 15 nM (Figure 2C). In the case of CENPN, the sgRNA and crRNA concentrations became saturated at ~2 and 5 nM, respectively (Figure 2D). However, even at the higher concentrations, the CENPN crRNA was less efficient than the corresponding sgRNA. Similarly to CENPN, the sgRNA against RELA was always more efficient than the corresponding crRNA, reaching maximum efficiency at a concentration of 2 nM compared with 10 nM for the crRNA (Figure 2E). However, in both cases, the knockout efficiency for RELA subsequently decreased at higher concentration for unknown reasons.

The above experiments tested a single guide sequence in each case. The targeting efficiency of a given RNA guide and the ability of a protein region to tolerate missense mutations may lead to reduced penetrance. One possible way to optimize the targeting efficiency is better guide sequence choice, which may be informed by comparing the performance of different RNA guides in various large-scale functional genomic screens, at least of genes that are required for optimal fitness. Alternatively, simultaneously targeting two distinct regions could potentially enhance the manifestation of the knockout phenotype through multiple DNA breaks within the same coding sequence. To test this, we evaluated the effect of combining 2 sgRNAs that target different sequences/regions of KIF11. We tested these sgRNAs either individually or combined at a final concentration of 15 nM and measured the mitotic index and fraction of mitotic cells with monopolar spindles. On the basis of these phenotypes, we did not detect a significant increase in knockout efficiency with the combined sgRNAs compared with the individual guides (Supplemental Figure S2).

Our results suggest that both sgRNAs and crRNAs are effective in promoting Cas9-mediated targeting and genome editing for gene knockouts, although the efficiency will vary depending on the specific gene target. Overall, the use of full-length sgRNA provides a faster and generally more robust and effective strategy for conducting this approach at lower RNA concentrations. For future studies, this relative effectiveness needs to be balanced by differences in cost due to the increased synthesis cost of the longer sgRNA.

Synthetic guides are effective for reverse transfection on printed arrays

The above experiments utilized standard transfection procedures to introduce the individual synthetic guide RNAs into Cas9-expressing cells. With the goal of developing strategies to conduct broader screening of cell biological phenotypes using CRISPR/Cas9-based inducible knockouts, we found that this transfection strategy can also be efficiently applied to a 96-well plate format (Supplemental Figure S2B). As an alternative large-scale strategy to analyze gene function, we also sought to test an array-based approach. Reverse transfection (Ziauddin and Sabatini, 2001) provides an alternative strategy for introducing oligonucleotides into cells. This approach involves placing a mixture of oligonucleotide and transfection reagent on a microscope slide and subsequently plating cells on the dried slide to allow them to proliferate on top of the transfection mixes. To test the effectiveness of reverse transfection for Cas9-based gene knockouts, the sgRNAs targeting KIF11, CENPN, and RELA were printed as arrays on microscope slides. In each case, the sgRNA sequences used correspond to those found to be effective by standard transfection (Figure 1). To detect the presence and location of the transfection complexes on the slide, a fluorescent dye-conjugated RNA was also added to the transfection mix before array printing. Each printed spot can encompass 50–100 cells, with the potential to print as many as 3200 spots on a single microscope slide. We compared the behavior of Cas9-expressing cells grown on spots printed with specific sgRNAs to neighboring cells grown on control spots without sgRNA. We found that the reverse transfection procedure was effective for creating the gene knockouts, with mitotic cells with monopolar spindles observed for KIF11 (Figure 3A) and protein depletion as

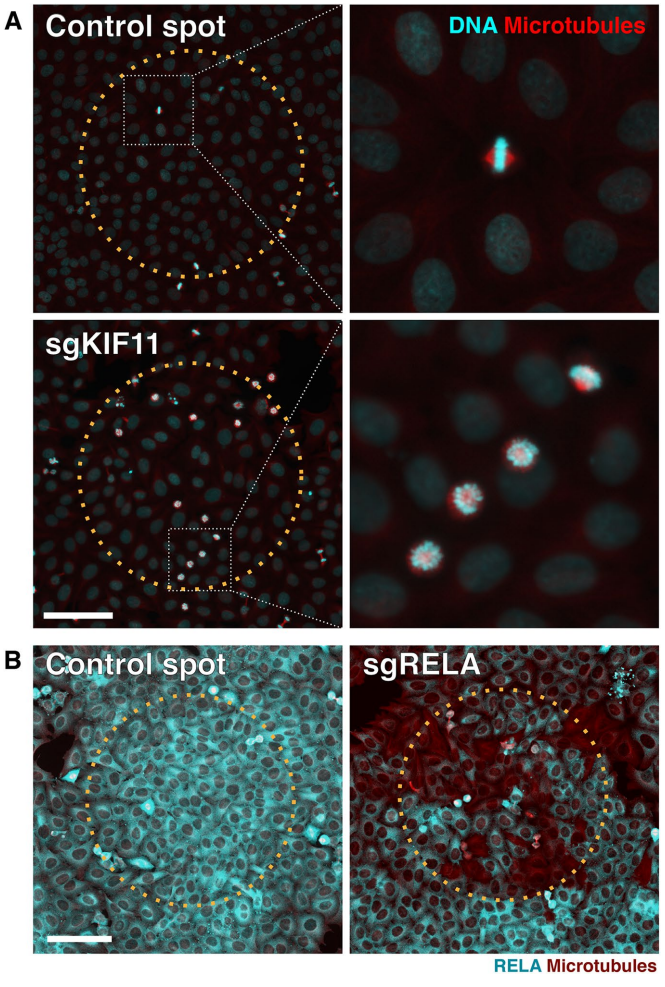

FIGURE 3: Reverse transfection allows efficient delivery of sgRNAs for phenotypic analyses. Immunofluorescence images of HeLa cells that were fixed and imaged 72 h postseeding on printed sgRNA array with control spots or spots containing sgRNA targeting KIF11 (A) or RELA (B). Cas9 expression in these cells was induced 12–18 h before seeding. For the KIF11 sgRNA array, cells were stained for DNA (cyan) and microtubules (red). Dotted boxes (white) indicate magnified region (right). For the RELA sgRNA array, cells were stained for RELA (cyan) and microtubules (red). In all images, the dotted circles (orange) indicate region of printed spot. Scale bar = 100 µm.

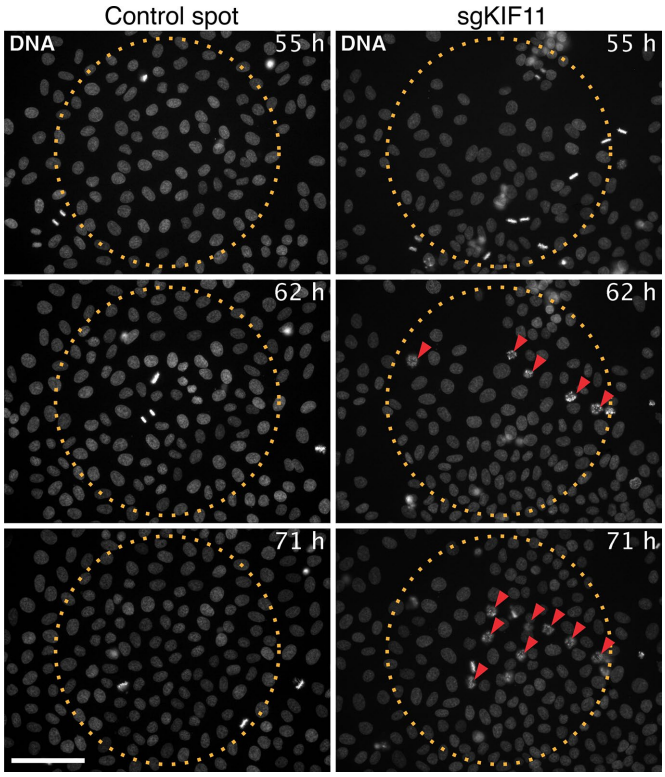

FIGURE 4: Reverse transfection allows real-time imaging of depletion phenotypes. Time-lapse stills of HeLa cells seeded on a printed sgRNA array with control spots (left) or spots containing an sgRNA targeting KIF11 (right). Spots were identified using a fluorescence dye-conjugated RNA (channel not shown). Cas9 expression in these cells was induced 12–18 h before seeding. Cells were stained for DNA and imaged in a heated microscope chamber at the indicated time postseeding. Dotted circles (orange) indicate the region of the printed spot. Red arrowheads highlight cells with monopolar spindles. Scale bar = 100 µm.

visualized by antibody staining for RELA (Figure 3B). Over the course of the experiment, clonal colonies expand beyond the area of the circled RNA spot and therefore cells displaying the knockout phenotype can also be detected outside of the circled region. Unfortunately, we were unable to detect a knockout phenotype for CENPN on the printed array (unpublished data). This could be due to the dilution of the guide RNA during the printing process, which may prevent robust CRISPR/Cas9 editing thus resulting an overall decrease in knockout efficiency.

To test the feasibility and effectiveness of the reverse transfection set-up to monitor depletion phenotypes in real time, we conducted live imaging of cells depleted of KIF11. Cells expressing Cas9 were grown on a printed array composed of control spots and spots containing the sgRNA against KIF11. After growth for 54 h, the cells were incubated with Hoechst to visualize DNA and imaged in a heated microscope chamber. Starting at 55 h postseeding, mitotic cells with monopolar spindles appeared within KIF11 sgRNA-containing spots, whereas cells on control spots continued to divide (Figure 4). These aberrant mitotic cells accumulated over time and were largely confined to the printed area. Our results show that the reverse transfection of synthetic guide RNAs on a printed array can be applied to live cell imaging to provide a more detailed temporal analysis of the phenotypic consequences of a gene knockout. Such an approach is also particularly advantageous when the time required for complete depletion of the target protein is not known.

Synthetic guide RNAs for robust cell biological analyses

In this study, we compared the efficacy of commercially available synthetic RNA guides and in vitro transcribed sgRNAs delivered using a standard transfection protocol developed for RNAi to cell lines stably expressing full-length sgRNA for their ability to induce CRISPR/Cas9-mediated knockout of three distinct gene targets. The cell line used in this study is a HeLa cell line, which is known to display aneuploidy. The aberrant copy number for a subset of genes may impact the overall knockout efficiency and this should generally be taken into consideration in the choice of the cell line, However, in this study, we are primarily focused on comparing the efficiency of various types of guide RNAs and their delivery methods. We find that synthetic sgRNA transfection can produce similar results to those obtained with stably expressed sgRNAs introduced via viral transduction. This approach allows for rapid knockout of a target gene in a population of cells and eliminates the need to generate a stable cell line expressing the targeting RNA. Although we did not detect significant improvement when combining two sgRNAs targeting KIF11, this has been reported to improve the knockout efficiency in other cases (Erard *et al.*, 2017). We found that synthetic crRNAs and in vitro transcribed sgRNAs are less potent than the corresponding full-length sgRNA but represent a cost-effective alternative to the more expensive synthetic sgRNAs for screening applications. We also observed differences in the timing of manifestation of the knockout phenotypes for each gene target, reflecting differences in Cas9 cutting and/or dynamics of gene turnover. Application of synthetic guide RNA concentrations ≥15 nM is generally most effective but in some cases further increases in RNA concentrations may lead to a reduction in knockout efficiency. Given that the synthetic guide RNA transfection approach can be easily adapted for screening applications, we demonstrated that this method is also successful with array-based reverse transfection when combined with immunofluorescence or live cell imaging.

MATERIALS AND METHODS

Cell culture and cell line generation

HeLa cells were maintained in DMEM supplemented with 100 U/ml streptomycin, 100 U/ml penicillin, 2 mM glutamine, and 10% (vol/vol) fetal bovine serum (FBS) and are tested for mycoplasma monthly. Cells were cultured at 37°C with 5% CO_2. The tetracycline-inducible Cas9 HeLa cell line (cTT20) was described previously (McKinley *et al.*, 2015). Single guide RNAs targeting KIF11 #1: GAAGTTAGTGTACGAACTGG (McKinley and Cheeseman, 2017); KIF11 #2: GGAACTTCACAACTTATTGG (cut-site 13,285 base pairs downstream of KIF11 #1, used in Supplemental Figure S2 only); CENPN: CCAGTACAAACCTACCTACG (McKinley *et al.*, 2015) and RELA: CTCGCCTGGGATGCTGCCCG were cloned into pLenti-sgRNA (puromycin resistant) (McKinley and Cheeseman, 2017) and introduced into the inducible Cas9 cell line by lentiviral transduction (Wang *et al.*, 2014, 2015).

Cas9 induction and cell transfection

Cells were seeded in media containing 1 mg/l doxycycline hyclate (Sigma) for >10 h before transfection. For transfection in a 12-well plate with 18-mm coverslips for immunofluorescence, the desired amounts of guide RNA and 2.5 µl Lipofectamine RNAi MAX (Invitrogen) were added to 250 µl of Optimem (Invitrogen) before vortexing and 15-min incubation at room temperature. The transfection mix was then applied to cells in 750 µl of fresh media for 24 h

before removal. RELA knockout experiments were carried out in six-well plates with doubled volumes. Cells were reseeded on 10-cm plates after 2 d for the FACS analysis. The KIF11 sgRNA transfection in 96-well plate was carried out with 0.25 µl Lipofectamine RNAi MAX and a final concentration of 25 nM sgRNA (Dharmacon) in 100 µl final total media volume. Exogenous guide RNAs target the same sequences as those used for lentiviral-derived stable cell lines described above. Synthetic guides (crRNA and sgRNA) were obtained from ThermoFisher and Dharmacon. crRNAs were hybridized/mixed with tracrRNA at a 1:1 ratio according to the manufacturer instructions. In vitro–transcribed sgRNAs were produced according to the manufacturer instructions using the Guide-it sgRNA In Vitro Transcription Kit (Takara). Doxycycline was refreshed every 24 h. For reverse transfection of cells on sgRNA arrays (prepared by Persomics; see below), cells were induced over night with 1 mg/l doxycycline hyclate before seeding on the array. Doxycycline was refreshed every 24 h. All experiments were performed at least twice. The mitotic index was determined by scoring the number of mitotic cells with condensed DNA and dividing by the total number of cells. Excess number of cells were scored per experiment to ensure accuracy. The exact sample sizes of each experimental condition are listed in Supplemental Table S1. Tukey's multiple comparison test was applied for the statistical comparisons of results between conditions using Prism 7 (Graphpad). Relative *p* values are listed in Supplemental Table S2 for the comparison of different conditions.

Immunofluorescence

Cells were fixed in 4% paraformaldehyde in PHEM (60 mM piperazine-*N*,*N*′-bis(2-ethanesulfonic acid) [PIPES], 25 mM HEPES, 10 mM ethylene glycol-bis(β-aminoethyl ether)-*N*,*N*,*N*′,*N*′-tetraacetic acid [EGTA], and 4 mM $MgSO_4$, pH 7) for analysis of KIF11 and CENPN phenotypes or phosphate-buffered saline (PBS) (for RELA) for 10 min at 37°C. DNA was stained with 5 mg/l Hoechst 33342 (Sigma). Microtubules were stained with mouse anti-tubulin DM1a at 1:2000 dilution when unconjugated or 1:500 dilution when conjugated to fluorescein isothiocyanate (FITC; Sigma). ab181981(Abcam) was used to stain for KIF11 at 1:500 dilution. Rabbit anti-RELA antibodies (D14E12; Cell Signaling) were used at 1:500 dilution. Images were acquired on a Nikon eclipse microscope equipped with a charge-coupled device (CCD) camera (Clara; Andor) using a Plan Fluor 40×/1.3 NA (KIF11 experiments) or Plan Fluor 20×/0.5 NA (rest) objective and appropriate fluorescence filters. Images for mitotic phenotypes were scaled nonlinearly to improve visibility. Identical adjustment for RELA and KIF11 signal were applied to all images when compared side by side. For Supplemental Figure S1, two to three z sections at 1-µm intervals were maximum projected before processing.

Flow cytometry

Cells were trypsinized before fixation in 2% paraformaldehyde in PBS for 10 min followed by incubation in 90% methanol in PBS overnight at –20°C. Cells were stained with Rabbit anti-RELA (D14E12; Cell Signaling) at 1:5000 followed by 1:1000 Cy2 AffiniPure Donkey Anti-Rabbit IgG (Jackson ImmunoResearch Laboratories). BD LSR II was used for flow cytometry and cell sorting and FlowJo (BD Biosciences) for data analysis.

sgRNA array

All fine chemicals were from MilliporeSigma. Array plates (Persomics USA) comprised a plate base of a 24 × 60 mm class I, 165- to 185-µm-thickness quartz glass wafer, embedded in a single-well black Society for Biomolecular Sciences–compliant microplate. Array plates were routinely coated with poly-L-lysine and air-dried prior to use. sgRNAs (obtained from Dharmacon) were resuspended in duplex buffer (IDT USA) and diluted to 12.5 µM before use. RNAs were suspended in an encapsulation mix, essentially as described (Genovesio *et al.*, 2011a,b), using red fluorescent nontargeting small interfering RNA as an optically addressable marker (red si-GLO; Dharmacon, USA) and a transfection agent. The encapsulation mix was composed of 165 mM sucrose, 0.085% (wt/vol) bovine gelatin type B, and 11% (vol/vol) transfection reagent. Printing was performed using a movable type array printer, where the print element for each condition was a sterile, disposable 330-µm-diameter borosilicate capillary (Persomics USA). Each capillary was filled with a single transfection mixture by capillary action and held in a print head magazine under a constant flow of >65–70% relative humidity sterile air. Arrays were contact printed onto poly-L-lysine–coated array plates with a contact time of 2500 ms. Post printing, arrays were air dried for 48 h and then stored at 5% relative humidity in an automated desiccator. All printing and production was performed in an ISO4 clean room.

Live cell imaging

Cells were imaged in CO_2-independent media (Invitrogen) and 0.1 mg/l Hoechst 33342 at 37°C. Images were acquired as for immunofluorescence on a Plan Fluor 20×/0.5 NA objective at intervals of 10 min.

ACKNOWLEDGMENTS

We thank the members of the Cheeseman laboratory and Heather Keys for support, input, and critical reading of the manuscript. This work was supported by grants from The Harold G. & Leila Y. Mathers Charitable Foundation and the National Institutes of Health (NIH)/National Institute of General Medical Sciences (GM088313 and GM108718) to I.M.C. and a grant from the NIH/National Human Genome Research Institute to Paul Blainey (HG009283).

REFERENCES

Cho SW, Kim S, Kim JM, Kim JS (2013). Targeted genome engineering in human cells with the Cas9 RNA-guided endonuclease. Nat Biotechnol 31, 230–232.

Cong L, Ran FA, Cox D, Lin S, Barretto R, Habib N, Hsu PD, Wu X, Jiang W, Marraffini LA, Zhang F (2013). Multiplex genome engineering using CRISPR/Cas systems. Science 339, 819–823.

Deltcheva E, Chylinski K, Sharma CM, Gonzales K, Chao Y, Pirzada ZA, Eckert MR, Vogel J, Charpentier E (2011). CRISPR RNA maturation by trans-encoded small RNA and host factor RNase III. Nature 471, 602–607.

Erard N, Knott SRV, Hannon GJ (2017). A CRISPR resource for individual, combinatorial, or multiplexed gene knockout. Mol Cell 67, 1080.

Genovesio A, Giardini MA, Kwon YJ, de Macedo Dossin F, Choi SY, Kim NY, Kim HC, Jung SY, Schenkman S, Almeida IC, *et al.* (2011a). Visual genome-wide RNAi screening to identify human host factors required for Trypanosoma cruzi infection. PLoS One 6, e19733.

Genovesio A, Kwon YJ, Windisch MP, Kim NY, Choi SY, Kim HC, Jung S, Mammano F, Perrin V, Boese AS, *et al.* (2011b). Automated genome-wide visual profiling of cellular proteins involved in HIV infection. J Biomol Screen 16, 945–958.

Jinek M, Chylinski K, Fonfara I, Hauer M, Doudna JA, Charpentier E (2012). A programmable dual-RNA-guided DNA endonuclease in adaptive bacterial immunity. Science 337, 816–821.

Jost M, Chen Y, Gilbert LA, Horlbeck MA, Krenning L, Menchon G, Rai A, Cho MY, Stern JJ, Prota AE, *et al.* (2017). Combined CRISPRi/a-based chemical genetic screens reveal that rigosertib is a microtubule-destabilizing agent. Mol Cell 68, 210–223.e216.

Mali P, Yang L, Esvelt KM, Aach J, Guell M, DiCarlo JE, Norville JE, Church GM (2013). RNA-guided human genome engineering via Cas9. Science 339, 823–826.

Mayer TU, Kapoor TM, Haggarty SJ, King RW, Schreiber SL, Mitchison TJ (1999). Small molecule inhibitor of mitotic spindle bipolarity identified in a phenotype-based screen. Science 286, 971–974.

McKinley KL, Cheeseman IM (2017). Large-scale analysis of CRISPR/Cas9 cell-cycle knockouts reveals the diversity of p53-dependent responses to cell-cycle defects. Dev Cell 40, 405–420.
McKinley KL, Sekulic N, Guo LY, Tsinman T, Black BE, Cheeseman IM (2015). The CENP-LN complex forms a critical node in an integrated meshwork of interactions at the centromere-kinetochore interface. Mol Cell 60, 886–898.
Morgens DW, Deans RM, Li A, Bassik MC (2016). Systematic comparison of CRISPR/Cas9 and RNAi screens for essential genes. Nat Biotechnol 34, 634–636.
Ruben SM, Dillon PJ, Schreck R, Henkel T, Chen CH, Maher M, Baeuerle PA, Rosen CA (1991). Isolation of a rel-related human cDNA that potentially encodes the 65-kD subunit of NF-kappa B. Science 251, 1490–1493.
Schmid RM, Perkins ND, Duckett CS, Andrews PC, Nabel GJ (1991). Cloning of an NF-kappa B subunit which stimulates HIV transcription in synergy with p65. Nature 352, 733–736.
Shalem O, Sanjana NE, Hartenian E, Shi X, Scott DA, Mikkelsen TS, Heckl D, Ebert BL, Root DE, Doench JG, Zhang F (2014). Genome-scale CRISPR-Cas9 knockout screening in human cells. Science 343, 84–87.
Shalem O, Sanjana NE, Zhang F (2015). High-throughput functional genomics using CRISPR-Cas9. Nat Rev Genet 16, 299–311.
Tzelepis K, Koike-Yusa H, De Braekeleer E, Li Y, Metzakopian E, Dovey OM, Mupo A, Grinkevich V, Li M, Mazan M, *et al*. (2016). A CRISPR dropout screen identifies genetic vulnerabilities and therapeutic targets in acute myeloid leukemia. Cell Rep 17, 1193–1205.
Wang T, Birsoy K, Hughes NW, Krupczak KM, Post Y, Wei JJ, Lander ES, Sabatini DM (2015). Identification and characterization of essential genes in the human genome. Science 350, 1096–1101.
Wang T, Wei JJ, Sabatini DM, Lander ES (2014). Genetic screens in human cells using the CRISPR-Cas9 system. Science 343, 80–84.
Wang T, Yu H, Hughes NW, Liu B, Kendirli A, Klein K, Chen WW, Lander ES, Sabatini DM (2017). Gene essentiality profiling reveals gene networks and synthetic lethal interactions with oncogenic ras. Cell 168, 890–903 e815.
Ziauddin J, Sabatini DM (2001). Microarrays of cells expressing defined cDNAs. Nature 411, 107–110.
Zimmermann M, Murina O, Reijns MAM, Agathanggelou A, Challis R, Tarnauskaite Z, Muir M, Fluteau A, Aregger M, McEwan A, *et al*. (2018). CRISPR screens identify genomic ribonucleotides as a source of PARP-trapping lesions. Nature 559, 285–289.